

# Ion temperature measurement on tokamak Golem

**Author:** Dario Cipciar

**Date:** 5.2.2021

Faculty of Science, Masaryk University, Department of electronics

---

## 1. Abstract

We attempted to systematically measure ion temperatures on tokamak Golem using a swept ball-pen probe. We have performed multiple discharges with different parameters and radial positions in order to find optimal conditions for measurement with ball-pen probe.

## 2. Experimental setup and data preparation

In this experimental campaign we have performed measurements of ion temperature ( $T_i$ ) and electron temperature ( $T_e$ ) using stationary electric probes at different radial positions during discharge in Ohmic (OH) regime. The tokamak was purged by a glow discharge in helium and was well prepared for  $T_i$  measurement. Data Acquisition System (DAS) was set to sampling frequency of 12.5 MHz. Coaxial cables had length of 8 m.

### 2.1. Discharge: #35346

Discharge parameters were at first set to:

Voltage on condenser batteries powering toroidal magnetic field coils:  $U_{Bt} = 1200$  V,

Current drive field source voltage:  $U_{CD} = 400$  V,

Current drive trigger delay:  $\tau_{CD} = 2000$  ms,

Requested gas pressure:  $p = 10$  mPa.

Probe tip position:  $R = 60$  mm.

The ball-pen probe (BPP) was biased with voltage of -150 to +150 V, at a sweeping frequency of 50 kHz. The Langmuir probe was in a floating regime. The schematic is shown on Fig. 1 The range of oscilloscope was set to 1 V. The discharge plasma parameters are shown on Fig. 2. The measured raw probe data are shown on Fig. 3. The raw signal suggests that the BPP did not operate correctly. However, after performing a discharge with BPP in a floating regime we have seen that BPP is intact and measuring. Thus, what we can observe on Fig. 3 is a superposition of stray current and a measured current. Stray currents are very large due to high sweeping frequency spreading through 8 m long coaxial cable. Signal clean-up procedure is applied to remove stray current. We use lowpass filter in order to

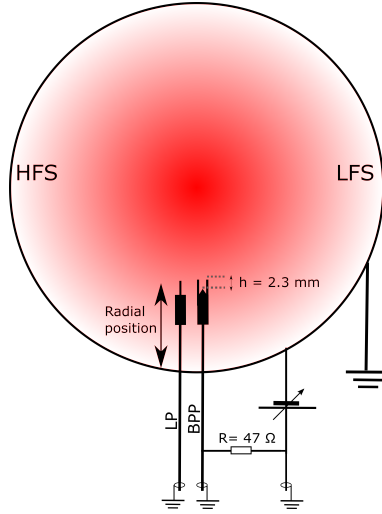


Figure 1: Simplified schematic of a probe setup. View of a tokamak plasma cross-section.

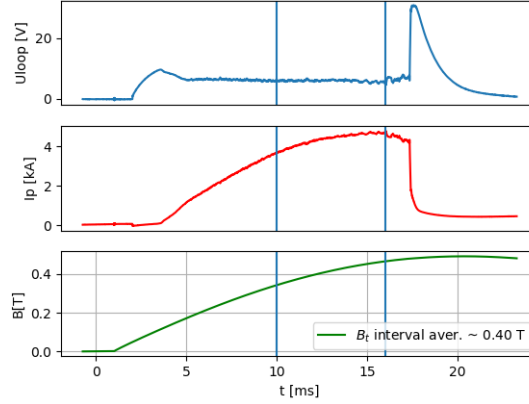


Figure 2: Plasma parameters, shot: 35346

remove structures with much higher frequency than the voltage sweeping frequency. The study of non-linear IV-characteristics with a sweeping frequency of E.g. 50 kHz requires that we measure also higher harmonics of this frequency. The upper bandwidth limit was set to 370 kHz, which allows to measure 7 harmonics. Lowpass filter alone will not remove the capacitive current. We can model the stray current as

$$I = C \frac{dU}{dt} + \text{offset}. \quad (1)$$

The capacity  $C$  can be obtained from slope of a linear dependency of the voltage derivative to current measured. Reconstructed stray current and offset is then subtracted from measured signal. Example of such signal clean-up procedure is shown on Figures 4, where the capacitive current is reconstructed and removed. On the same figure we can see, that some stray current, although 100x lower in amplitude, still remains. This current shown in red on Fig. 4 is in comparison to previously reconstructed current shifted in phase by  $\pi/2$ . We can repeat the same signal clean-up procedure, as shown on Fig. 5, however this time we need to compensate for the phase shift (shown on upmost sub-figure). The second capacitive current is removed and as shown on Fig. 6 the lowpass filter is applied. We can see that the amplitude of stray current decreased to 1/200 of it's initial amplitude.

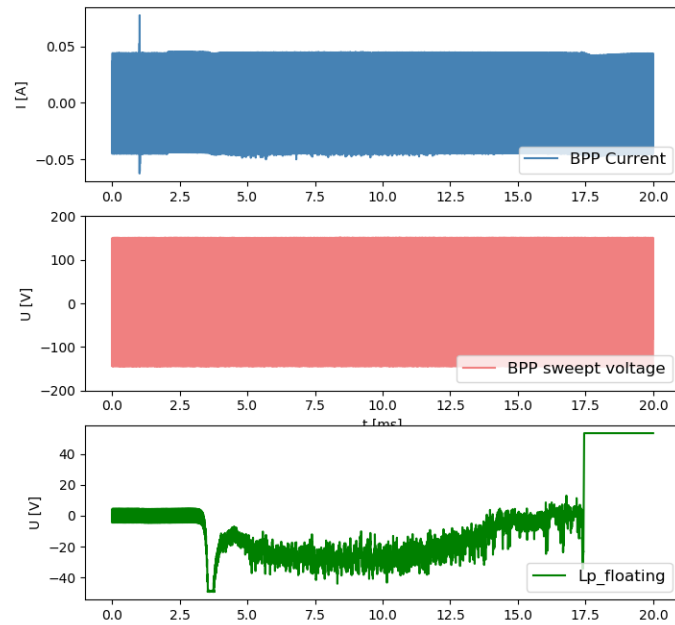


Figure 3: Raw signal from probes, shot: 35346

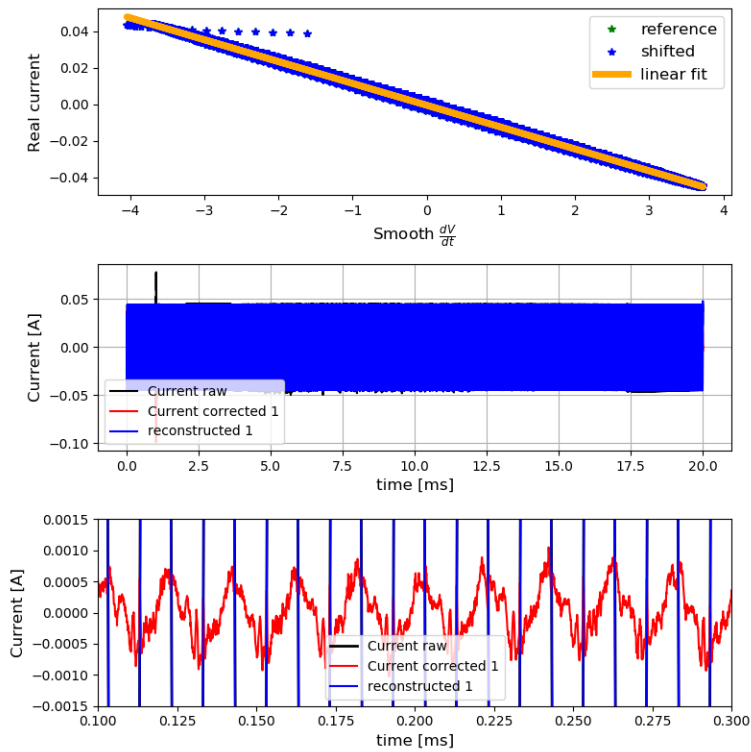


Figure 4: First stray current reconstruction and removal, shot: 35346

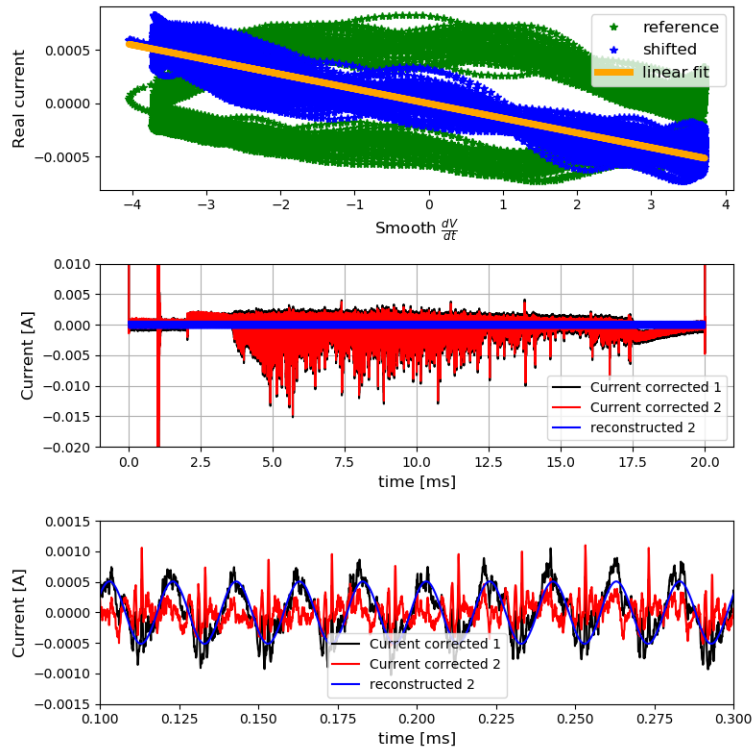


Figure 5: Second stray current reconstruction and removal, shot: 35346

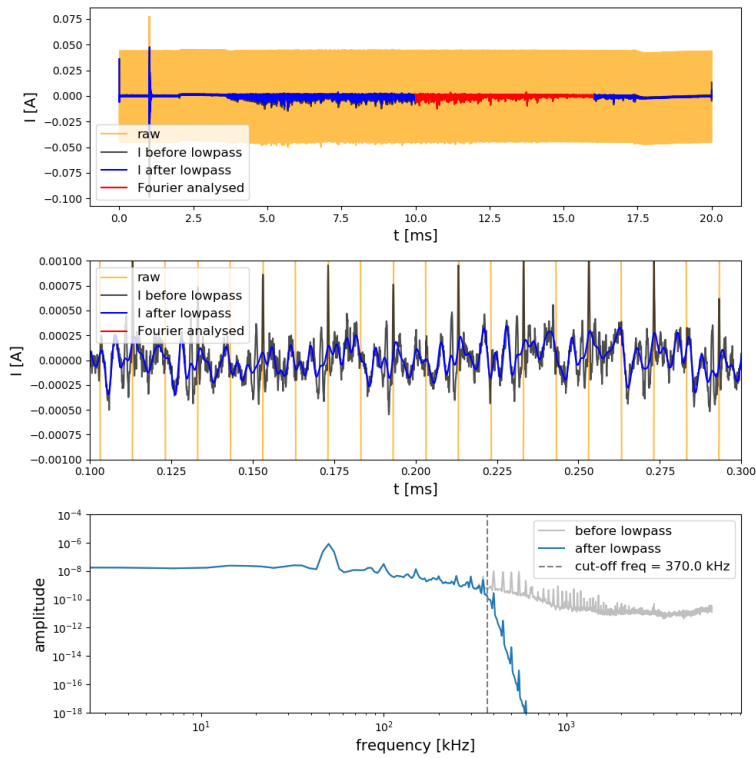


Figure 6: Filtering and a Fourier analysis of signal, shot: 35346

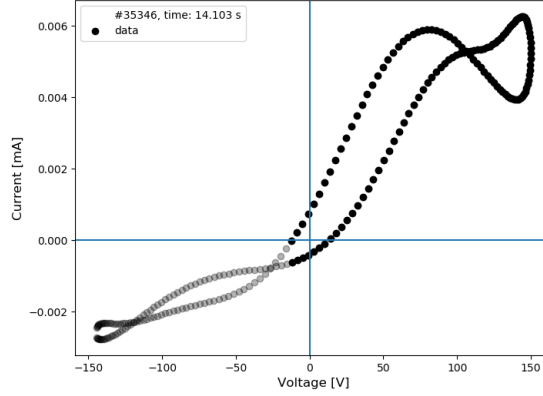


Figure 7: Ramp-up and ramp-down hysteresis of IV-characteristics before secondary clean-up, shot: 35346

After the signal clean-up we can separate the signal into individual I-V characteristics. We observe a hysteresis in the I-V characteristics over one sweep period. Similar hysteresis was observed with Langmuir probes swept at frequencies in order of tens kHz, when the hysteresis was caused by the resistive-capacitive impedance of the flux tube. However, for Langmuir probe swept at frequencies in order of 100 kHz the hysteresis appears on the electron saturation side, which would be caused by capacitive coupling of the flux tube to the magnetic field lines [2]. The appearance of I-V characteristics hysteresis on BPP was not yet observed nor explained. We may dispute that similar effect or combination of above mentioned effects could cause the hysteresis (shown on Fig. 7). The capacitive coupling caused by the resistive-capacitive impedance of the flux tube can be suppressed by the mentioned procedure. We can reconstruct the capacitive current from current measured before plasma is created. However, if in fact the hysteresis occurs due to coupling of the flux tube to the magnetic field lines the described clean-up procedure is ineffective. We observe that even though the capacitive coupling was to a great extent suppressed, the hysteresis still remains or is suppressed as well. We also need to take into account possible changes in the vertical and horizontal position of the plasma.

I-V characteristics can be fitted from the plasma potential  $V_p$  using a 4-parameter fit. Since magnitude of the magnetic field was changing during the whole discharge we have used the unweighted method for fitting the I-V characteristics. The formula used for 4-parameter fitting is:

$$I(V) = \exp(\alpha_{\text{BPP}}) I_{\text{sat}}^+ [1 + R(V - \Phi)] - I_{\text{sat}}^+ \exp((\Phi - V)/T_i). \quad (2)$$

The fitting parameters obtained are the ion temperature ( $T_i$ ), plasma potential ( $\Phi$ ), ion saturation current ( $I_{\text{sat}}^+$ ) and linear increase of electron current is described by slope ( $R$ ).

For the coefficient  $\alpha_{\text{BPP}}$  we have created an empirical relation (viz. Fig. 9) based on measurements of BPP I-V characteristics for different toroidal magnetic fields at Golem (viz. Fig. 8). Note that measurement at  $B_t = 0.5$  T was excluded from derivation of empirical relation. The resulting empirical relation is:

$$\alpha_{\text{BPP}}(t) = \ln\left(\frac{I_{\text{sat},e}}{I_{\text{sat},i}}\right) = (-2.7 \pm 0.5) \cdot B_t(t) + (2.04 \pm 0.2) \quad (3)$$

Examples of 4-parameter fits of measured I-V characteristics in 35346 are shown on Fig. (10 - 12), where for  $B_t(t)$  we have used an interpolated value of  $B_t$  for each (10 $\mu$ s) interval of an ion temperature measurement.

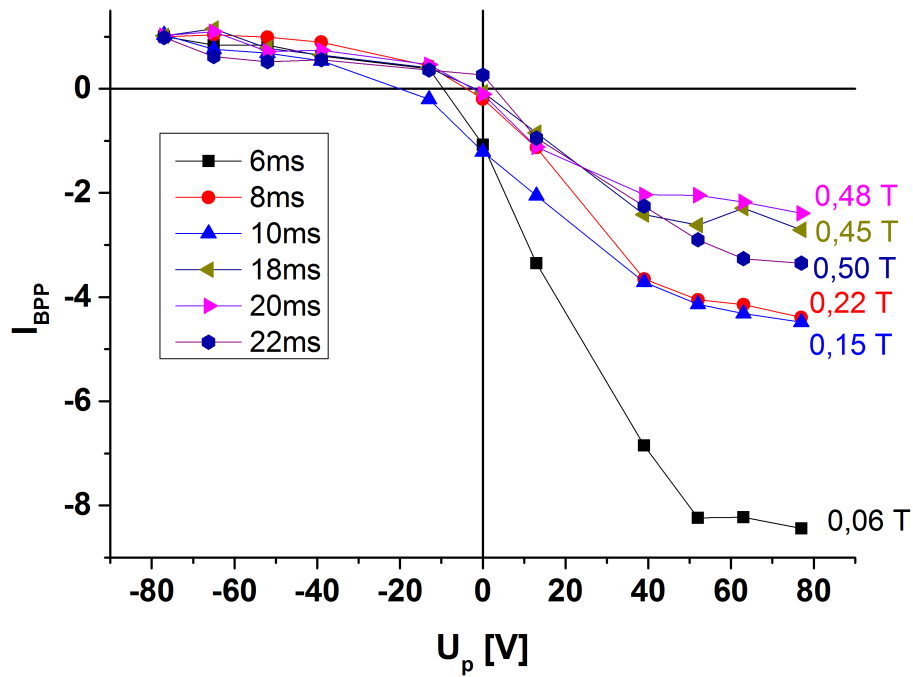


Figure 8: Measured BPP I-V characteristics on tokamak Golem, where  $I_{BPP}$  is normalised to 1 [1].

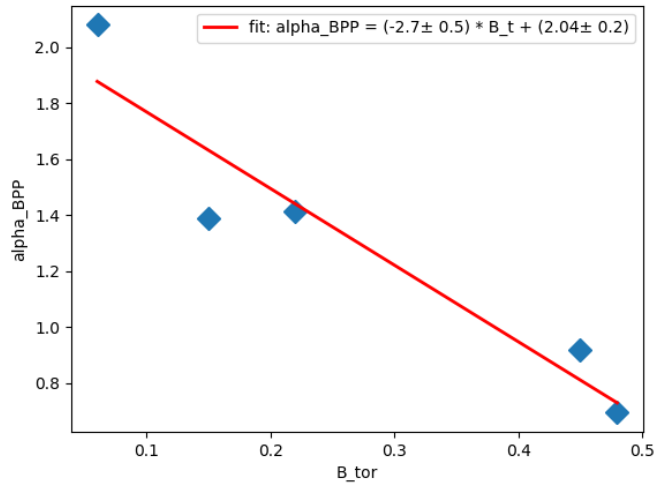


Figure 9: Empirical derivation of calibration relation (3).

In order to create a temporal profile of ion temperature with defined level of uncertainty we set filtering criteria as follows:

$$T_{i,err}/T_i > 0.6,$$

$$V_{p,err}/V_p > 0.6,$$

$$T_i < (V_{peak} - V_p)/1,$$

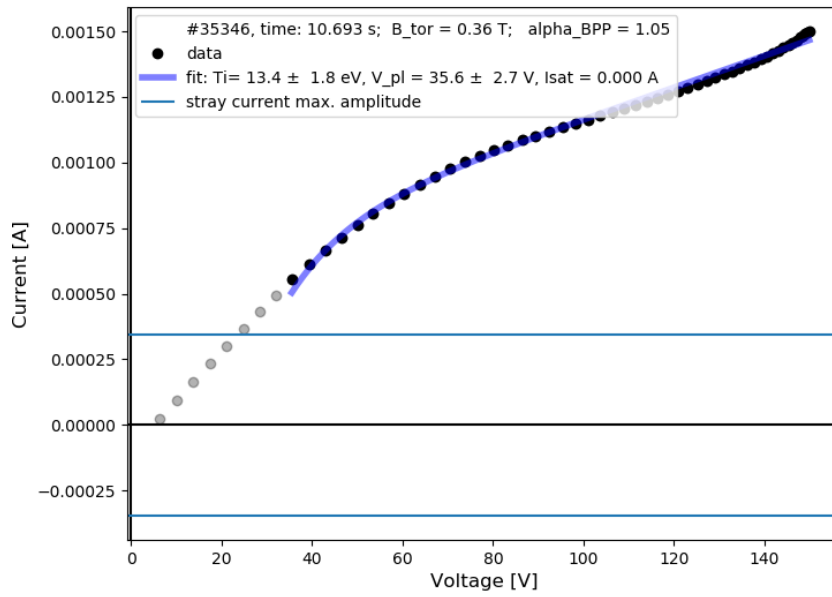


Figure 10: Example of 4-parameter fit of the electron branch, shot: 35346

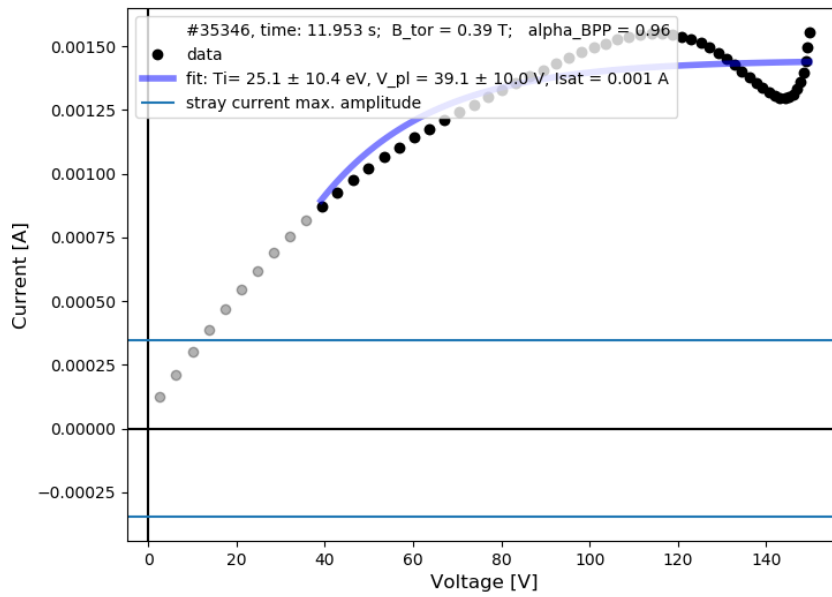


Figure 11: Example of 4-parameter fit of the electron branch, shot: 35346

where  $V_{\text{peak}} = 150 \text{ V}$  is the peak value of voltage applied on the BPP. The resulting temporal profile is shown on Fig. 13.

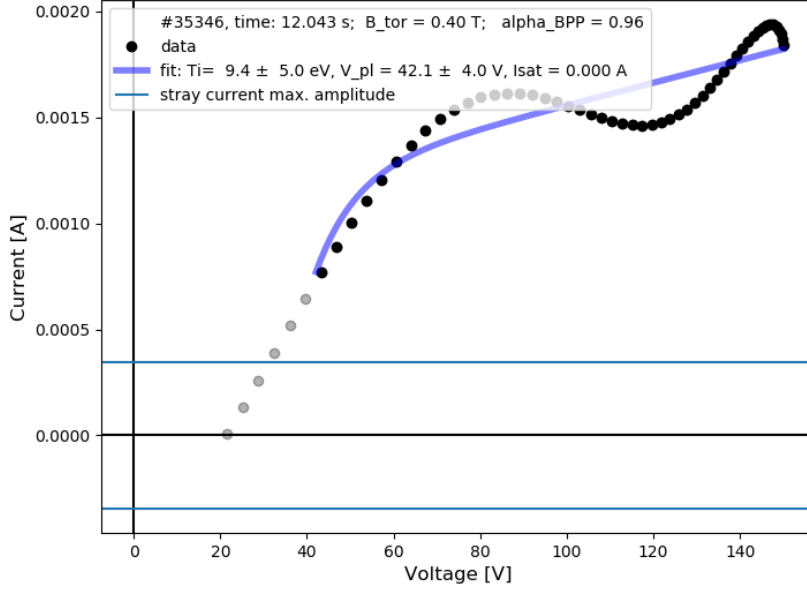


Figure 12: Example of 4-parameter fit of the electron branch, shot: 35346

## 2.2. Discharge: #35346: Cutoff refit procedure and demonstration

The primary goal of Cutoff fitting technique is to increase the number of 4-parameter fits which satisfy the filtering criteria mentioned above. Secondary purpose is to prove that ion temperature can be obtained from exponential part of I-V's electron branch within a fitting interval  $(V_{\text{peak}} - V_p)/T_i \geq 1$  (Ion saturation current decays to at least  $e^{-1}$  of the original amplitude) and the ion temperature does not change with the increment of voltage applied. For example if we use an amplitude of swept voltage  $U_{\text{peak}} = 80$  V and the plasma potential  $U_p = 30$  V the highest ion temperature that we can obtain is 50 eV, if we measure on the given interval  $T_i = 30$  eV, the ion temperature should remain constant if we increase the voltage amplitude. However, due to turbulence in plasma which autocorrelation time in order of  $10\mu\text{s}$  parts of the measured I-V characteristics can be disrupted. If the disruption happens at the end of I-V characteristics the fit can converge to an mediate ion temperature of the turbulence and be discarded by the filtering criteria. This often observed phenomenon can be overcome by an cutoff refit procedure as shown on Fig. (32 - 34). We apply the cutoff fitting to I-V characteristics which did not pass the filtering criteria mentioned before. This robust technique sequences the I-V characteristic into voltage intervals and performs the 4-parameter fit starting at plasma potential until cutoff voltage for each interval. The voltage interval step is not given by a constant voltage increment, but rather given by a constant increment of data points. Note that the skew of this particular approach is taken into account when we preform the numerical derivative described below. For the purpose of this work I have chosen to perform a fit for each 3 data points. We have tested and confirmed the independence of this parameter on the resulting distribution. The routine takes into account the fitting interval  $(V_{\text{peak}} - V_p)/T_i \geq 1$  and does not converge if his criterion is not satisfied. All the results of individual fits are stored, while the results which satisfy:  $T_{i,\text{err}}/T_i > 0.6$  are passed to numerical approximation of the derivative (forward difference), given as :

$$\text{difference} = \frac{T_i[j+1] - T_i[j]}{U_{\text{cutoff}}[j+1] - U_{\text{cutoff}}[j]}. \quad (4)$$



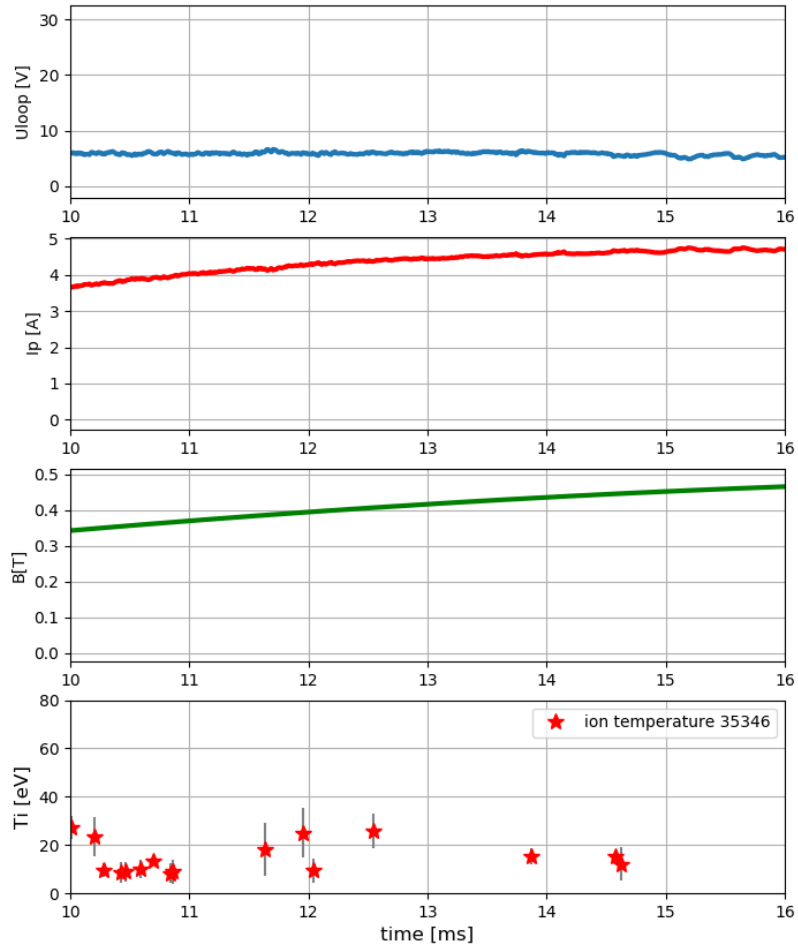


Figure 13: The temporal profile of  $T_i$ , #35346,  $R = 60$  mm

The absolute value of difference which is closest to 0 and satisfies empirical criterion  $|difference| < 0.5$  is considered the plateau where the results are constant. Since numerical derivative can be calculated for either of the two following results (forward / backward difference) and we assume that the results of the two following fits are almost identical we have placed the derivative "in between" and we choose the fit with lower variance for the final result. The resulting temporal profile is shown on Fig. 14.

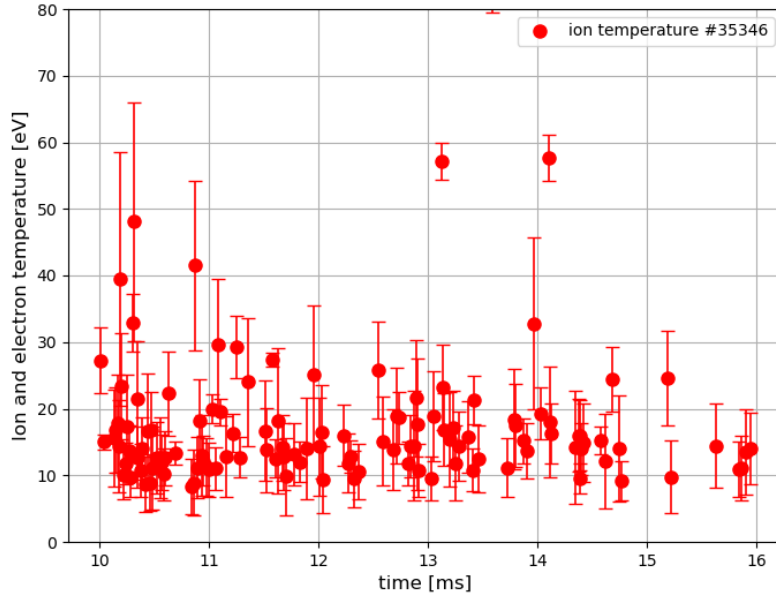


Figure 14: The temporal profile of  $T_i$  created using cutoff refit procedure, #35346,  $R = 60$  mm

### 2.3. Discharge: #35362

Discharge parameters were set to:

Voltage on condenser batteries powering toroidal magnetic field coils:  $U_{Bt} = 800$  V,

Current drive field source voltage:  $U_{CD} = 400$  V,

Current drive trigger delay:  $\tau_{CD} = 2000$  ms,

Requested gas pressure:  $p = 10$  mPa.

Probe tip position:  $R = 55$  mm.

The ball-pen probe (BPP) was biased with voltage of -150 to +150 V, at a sweeping frequency of 50 kHz. The plasma parameters are shown on Fig. 15 The clean-up procedure was applied as shown of Fig. (16, 17 and 18 ).

Similarly to previous discharge the IV-characteristics show hysteresis. Examples are shown of Fig. 35 and Fig. 36 The results are shown on Fig. 19 and the results of cutoff procedure on Fig. 20

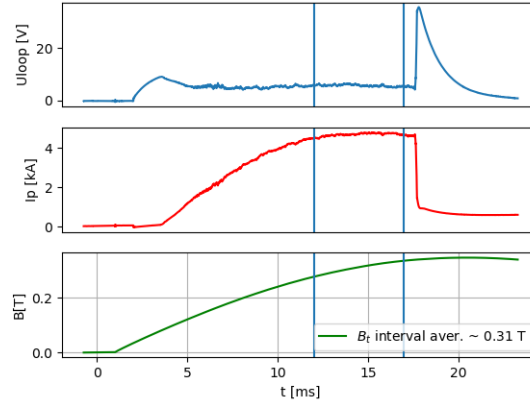


Figure 15: Plasma parameters with highlighted region for ion temperature measurement, shot: 35362

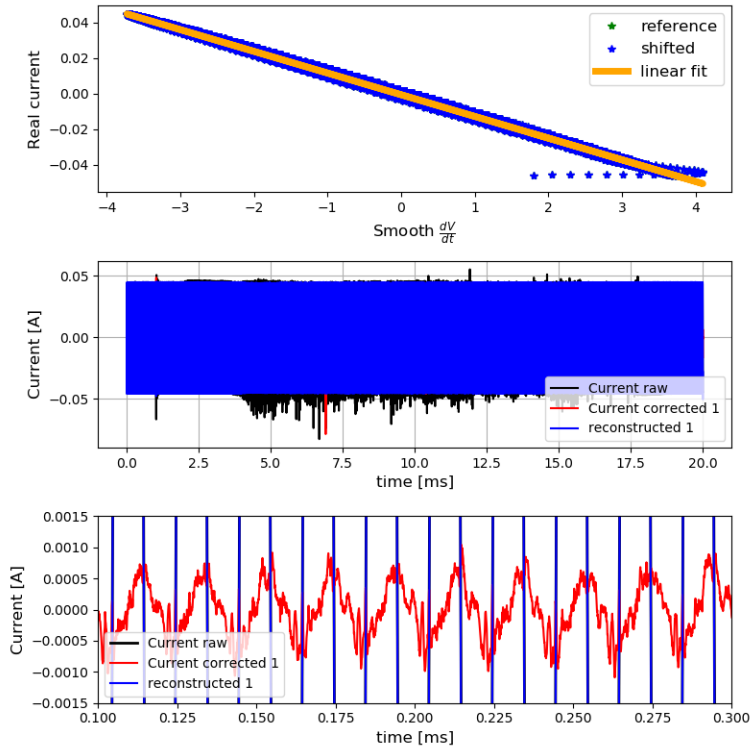


Figure 16: First stray current reconstruction and removal, shot: 35362

## 2.4. Discharge: #35364

Discharge parameters were set to:

Voltage on condenser batteries powering toroidal magnetic field coils:  $U_{Bt} = 800$  V,

Current drive field source voltage:  $U_{CD} = 400$  V,

Current drive trigger delay:  $\tau_{CD} = 2000$  ms,

Requested gas pressure:  $p = 10$  mPa.

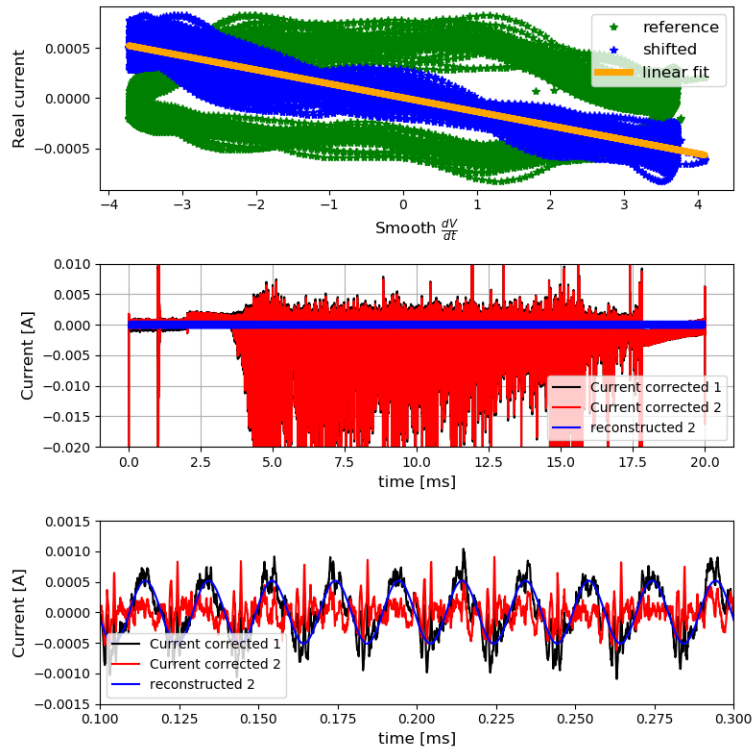


Figure 17: Second stray current reconstruction and removal, shot: 35362

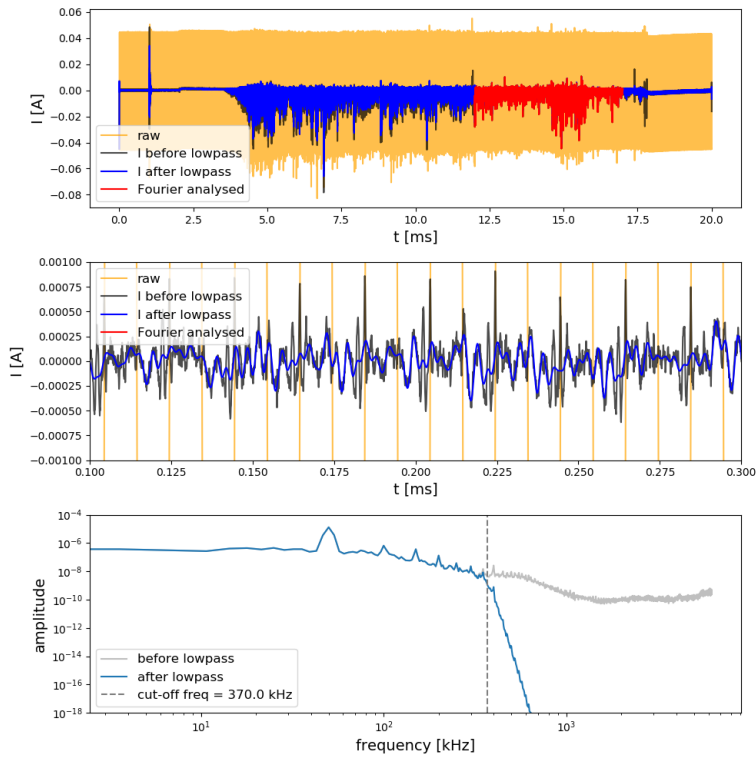


Figure 18: Filtering and a Fourier analysis of signal, shot: 35362

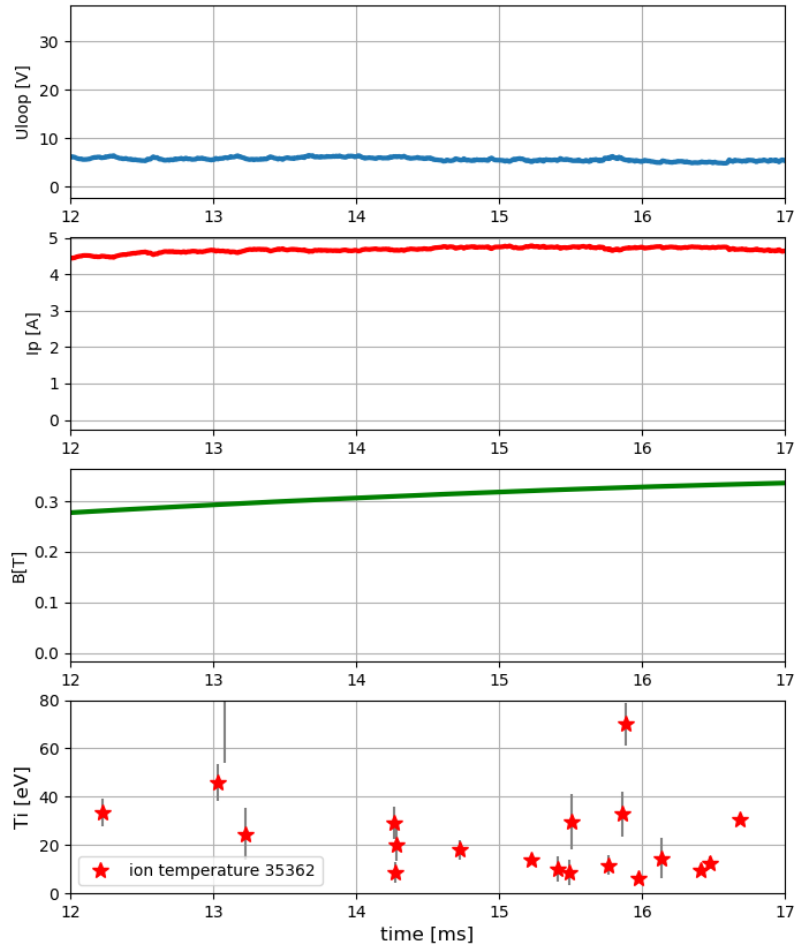


Figure 19: The temporal profile of  $T_i$ , #35362,  $R = 55$  mm

Probe tip position:  $R = 65$  mm.

The ball-pen probe (BPP) was biased with voltage of -150 to +150 V, at a sweeping frequency of 50 kHz. The plasma parameters are shown on Fig. 21 The clean-up procedure was applied as shown of Fig. (22, 23 and 24 ).

Similarly to previous discharge some of the IV-characteristics show hysteresis. Examples are shown of Fig. 37 and Fig. 39 The results are shown on Fig. 25 and the results of cutoff procedure on Fig. 26

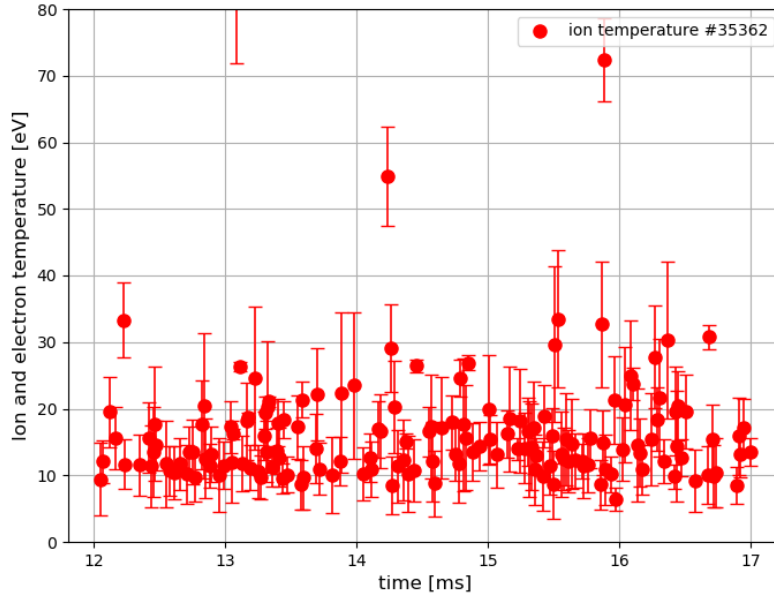


Figure 20: The temporal profile of  $T_i$  created using cutoff refit procedure, #35362,  $R = 55$  mm

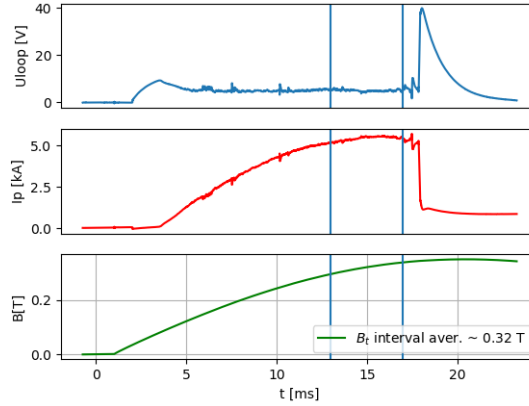


Figure 21: Plasma parameters with highlighted region for ion temperature measurement, shot: 35364

## 2.5. Discharge: #35366 - 10 kHz sweeping frequency

Discharge parameters were set to:

Voltage on condenser batteries powering toroidal magnetic field coils:  $U_{Bt} = 800$  V,

Current drive field source voltage:  $U_{CD} = 400$  V,

Current drive trigger delay:  $\tau_{CD} = 2000$  ms,

Requested gas pressure:  $p = 10$  mPa.

Probe tip position:  $R = 67.5$  mm.

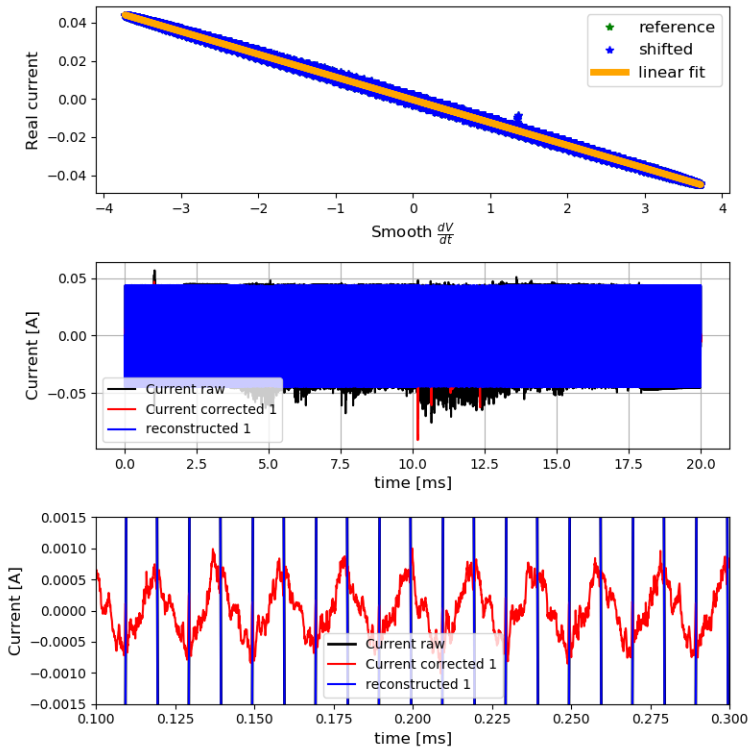


Figure 22: First stray current reconstruction and removal, shot: 35364

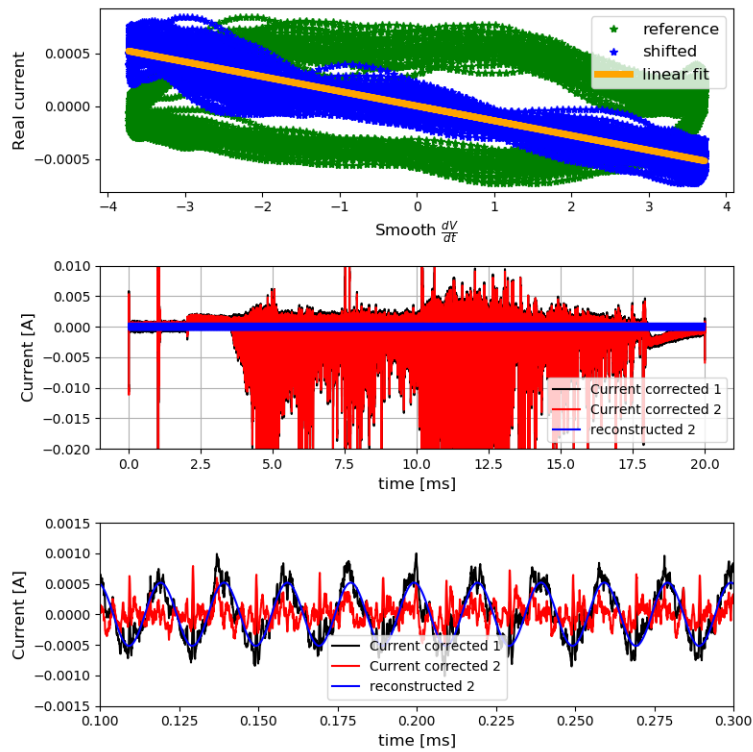


Figure 23: Second stray current reconstruction and removal, shot: 35364

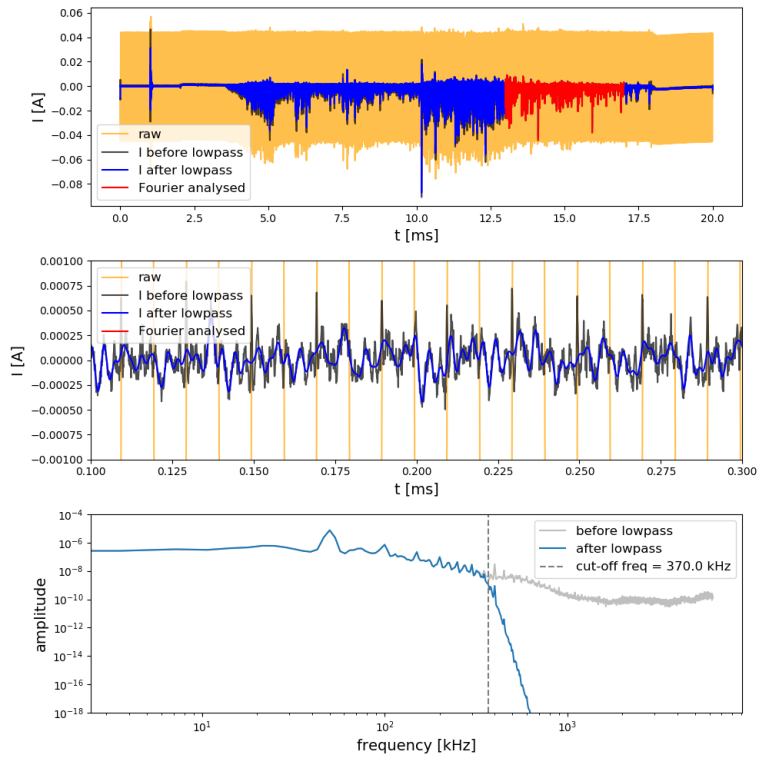


Figure 24: Filtering and a Fourier analysis of signal, shot: 35364

The ball-pen probe (BPP) was biased with voltage of -150 to +150 V, at a sweeping frequency of 10 kHz. The plasma parameters are shown on Fig. 27 The clean-up procedure was applied as shown of Fig. (28, 29 and 30 ).

The results of cutoff procedure on Fig. 31



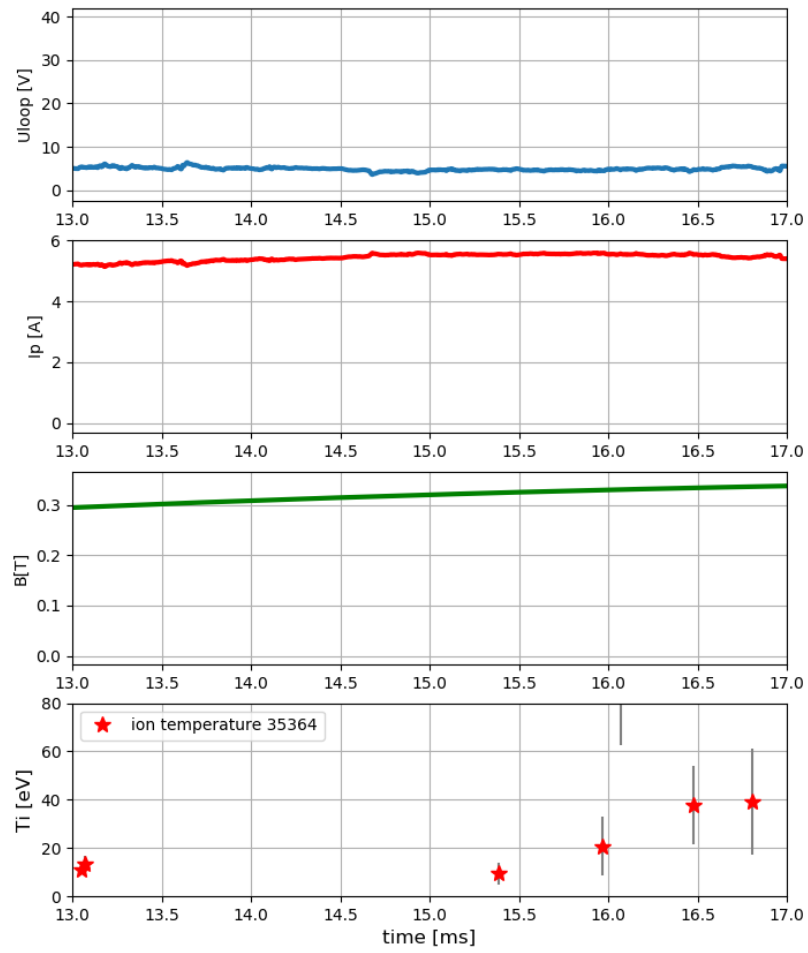


Figure 25: The temporal profile of  $T_i$ , #35362,  $R = 65$  mm

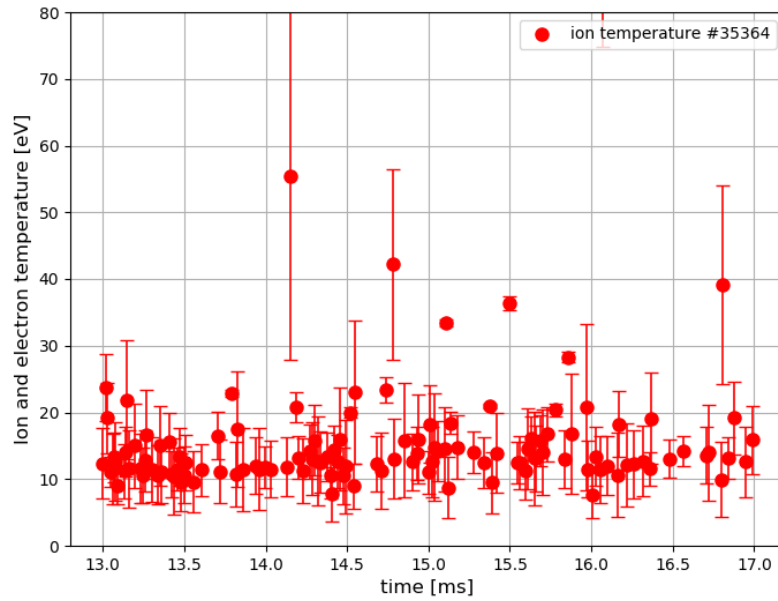


Figure 26: The temporal profile of  $T_i$  created using cutoff refit procedure, #35364,  $R = 65$  mm

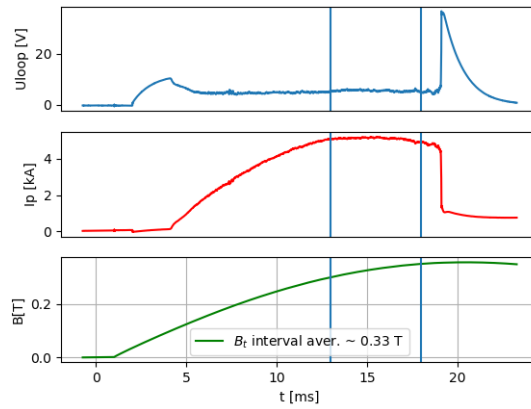


Figure 27: Plasma parameters with highlighted region for ion temperature measurement, shot: 35366

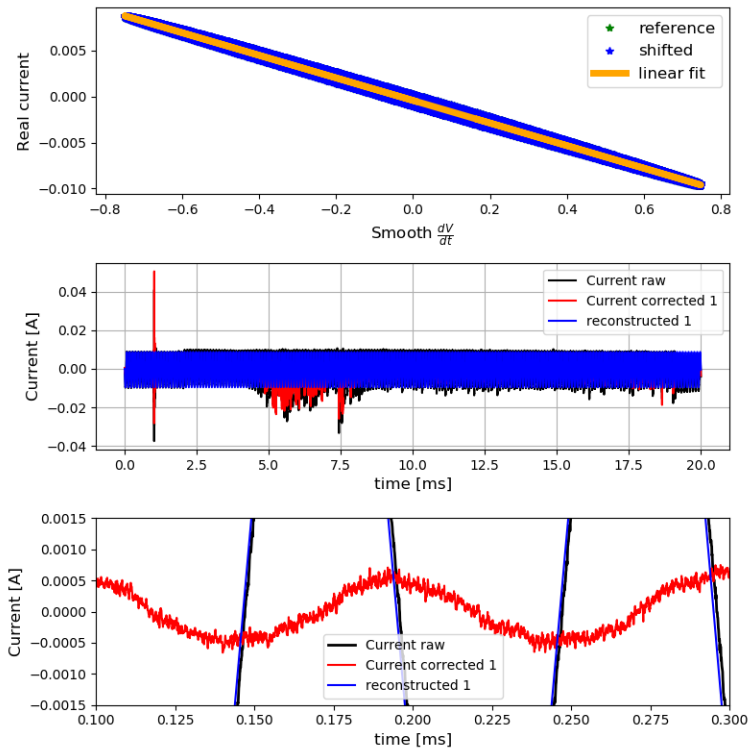


Figure 28: First stray current reconstruction and removal, shot: 35366

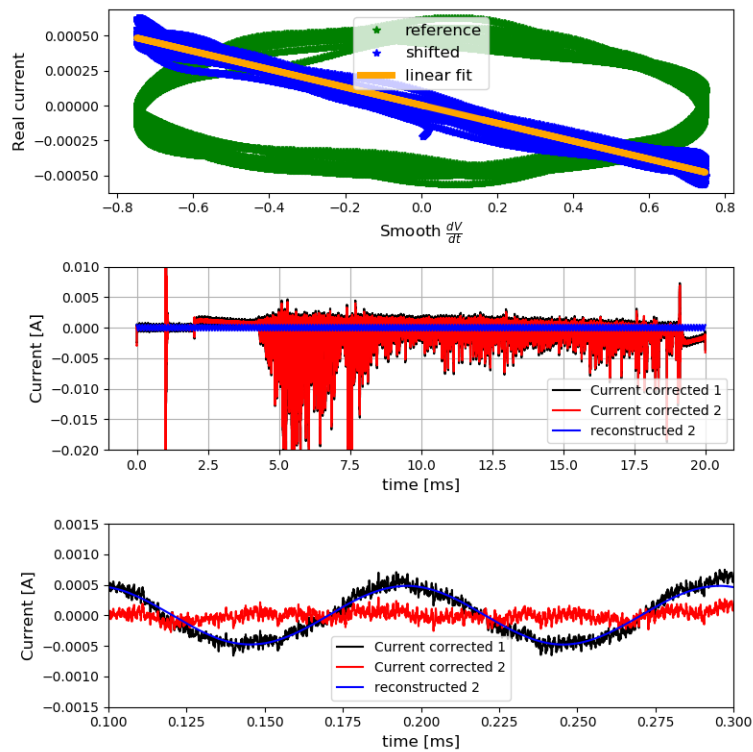


Figure 29: Second stray current reconstruction and removal, shot: 35366

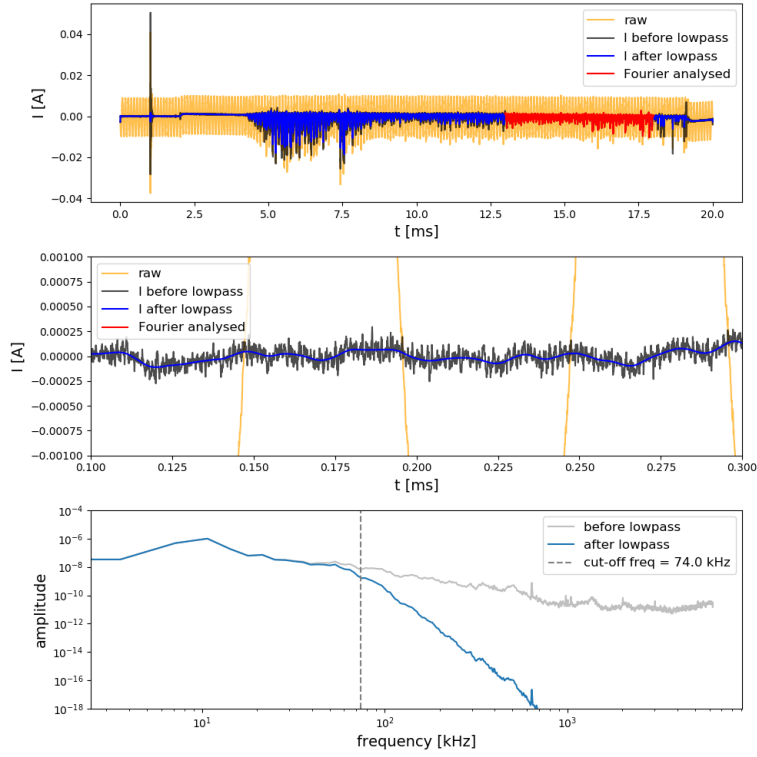


Figure 30: Filtering and a Fourier analysis of signal, shot: 35366

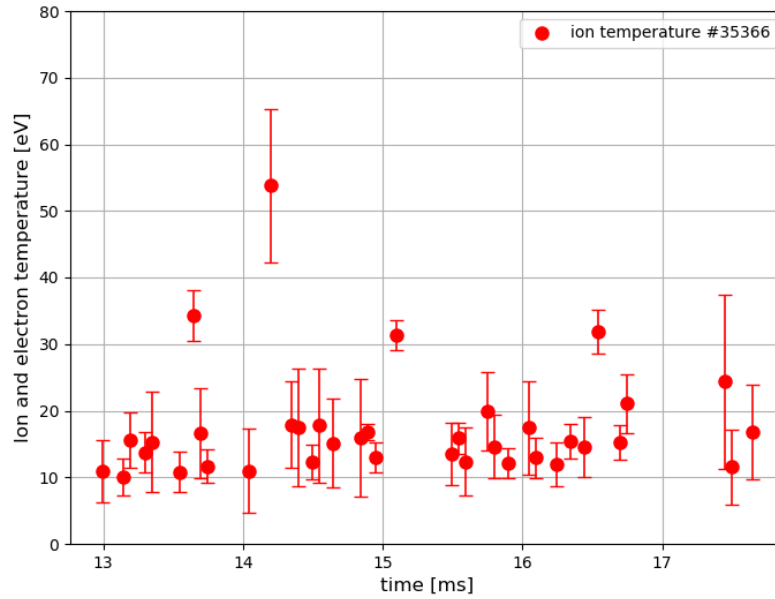


Figure 31: The temporal profile of  $T_i$  created using cutoff refit procedure, #35366,  $R = 67.5$  mm

# Conclusion

Using Ball-pen probe we were able to measure the ion temperature during multiple discharges at different radial positions. In this experimental campaign we have used new high voltage amplifier WMA-100 which made sweeping possible from -150 V up to +150 V with frequency of 50 kHz. Also an enormous improvement was DAS with sampling frequency of 12.5 MHz. The capacitive current created in coaxial cables in this experimental campaign was higher than in previous campaigns. This was probably caused by increased length of coaxial cables.

During discharge analysis we have improved the stray current removal by adding a secondary removal of stray currents with phase shift equal to 90 degrees. This current could be caused by reflection of signal at the end of coax cable or at connectors (or possible inductance). We have developed a script for cutoff refitting of failed fits which can increase the yield of fits which satisfy filtering criteria from 5 % up to 30 %. The ion temperature results at radial positions of  $R = 55, 60, 65$  mm show almost identical results with near normal distribution peaking at temperature 15 eV. However, the position of plasma relative to position of probe is not constant according to calculations from Mirnov coil data. Most critical time period when the plasma is changing position appears to be 14-18 s, which is exactly the period when  $T_i$  measurement takes place. We have observed hysteresis on I-V characteristics in all the discharges during this experimental campaign. Hysteresis in the steep part of the I-V could be explained as an effect of leftover capacitive current. However, hysteresis in the electron saturation part needs more elaborate explanation. We have seen that in many cases the electron current with increasing voltage applied did not increase nor saturate (as our model predicts) and thus created a hysteresis loop in the electron saturation part. This problem leads to a failure of most attempts to fit the curve from plasma potential until +150 V. We have shown that fitting the I-V characteristics from plasma potential until sufficient "cutoff" voltage  $\approx 150$  V can deliver up to 5 times more results with the same distribution.

In the next experimental campaign we could attempt to shorten the coaxial cables in order to reduce stray current. Keeping the DAS ground galvanically isolated is necessary for reduction of cross-talk currents originating in other diagnostics and proves crucial to this measurement. Also I would suggest keeping the parameter  $U_{Bt} = 1200$  V, although it will reduce the apparent effective signal by symmetrizing the BPP I-V characteristic. Amplitude of swept voltage of 150 V proved to be sufficient, since the maximum (credible)  $T_i = 40$  eV was observed. In order to minimize stray currents while reaching highest possible temporal resolution I would suggest sweeping 0 to +120 V in the next measurement. In order to obtain electron temperatures with precision the secondary repeated discharge with floating BPP and LP proved to be most useful.

# Bibliography

- [1] P. Mácha, Edge plasma parameter measurements of the GOLEM tokamak using ball-pen and Langmuir probe. Bachelor thesis, ČVUT, 2018.
- [2] P. Verplancke, Langmuir probes at high frequencies in a magnetized plasma. Dissertation, University of Ghent, 1996.

# Appendix

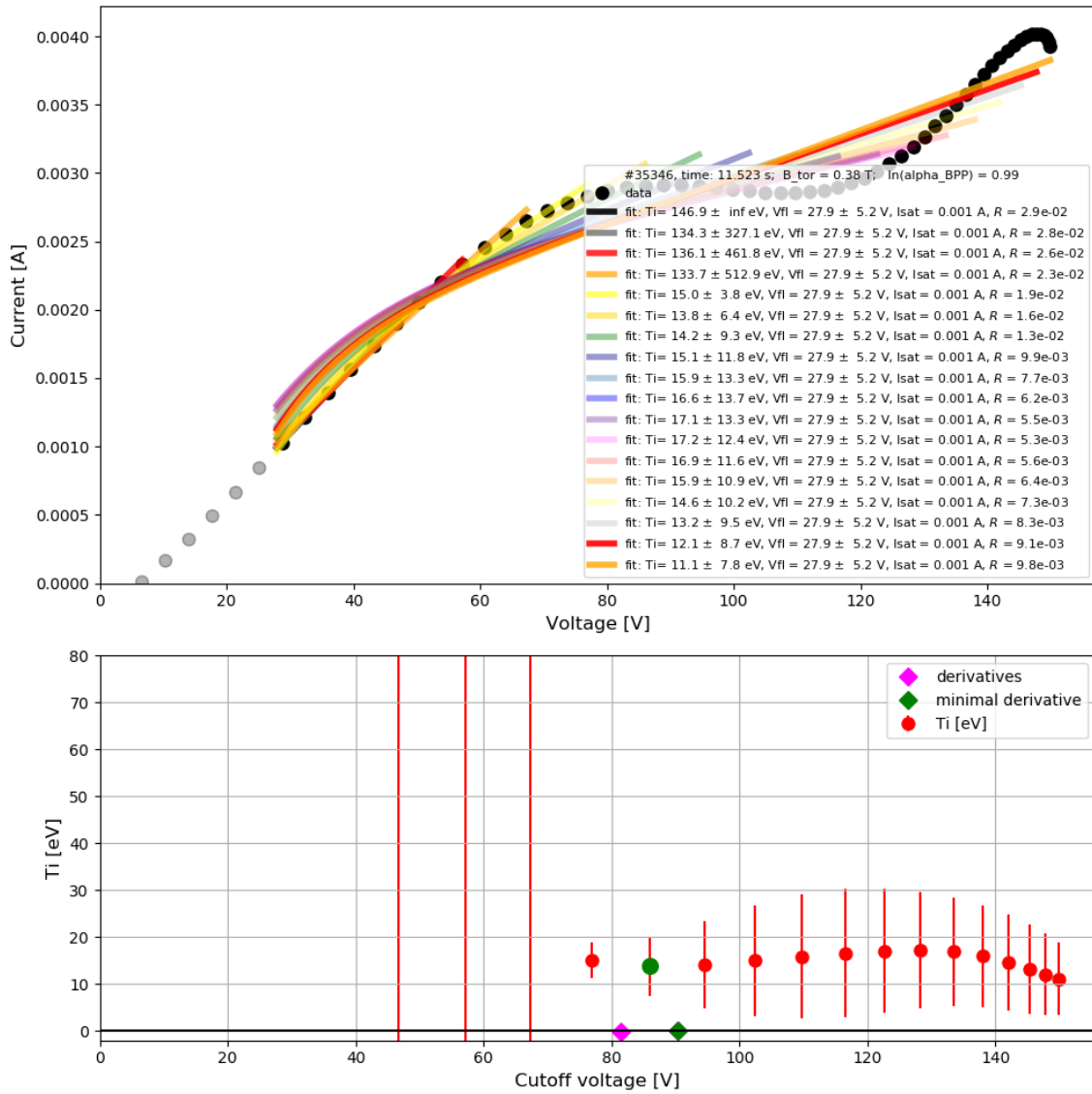


Figure 32: Example of cutoff 4-parameter fit of the electron branch. Top: Graphical representation of the fitting routine. Bottom: Summary of fitting results and their derivatives. Green color marks the resulting  $T_i$  and the lowest derivative, shot: 35346

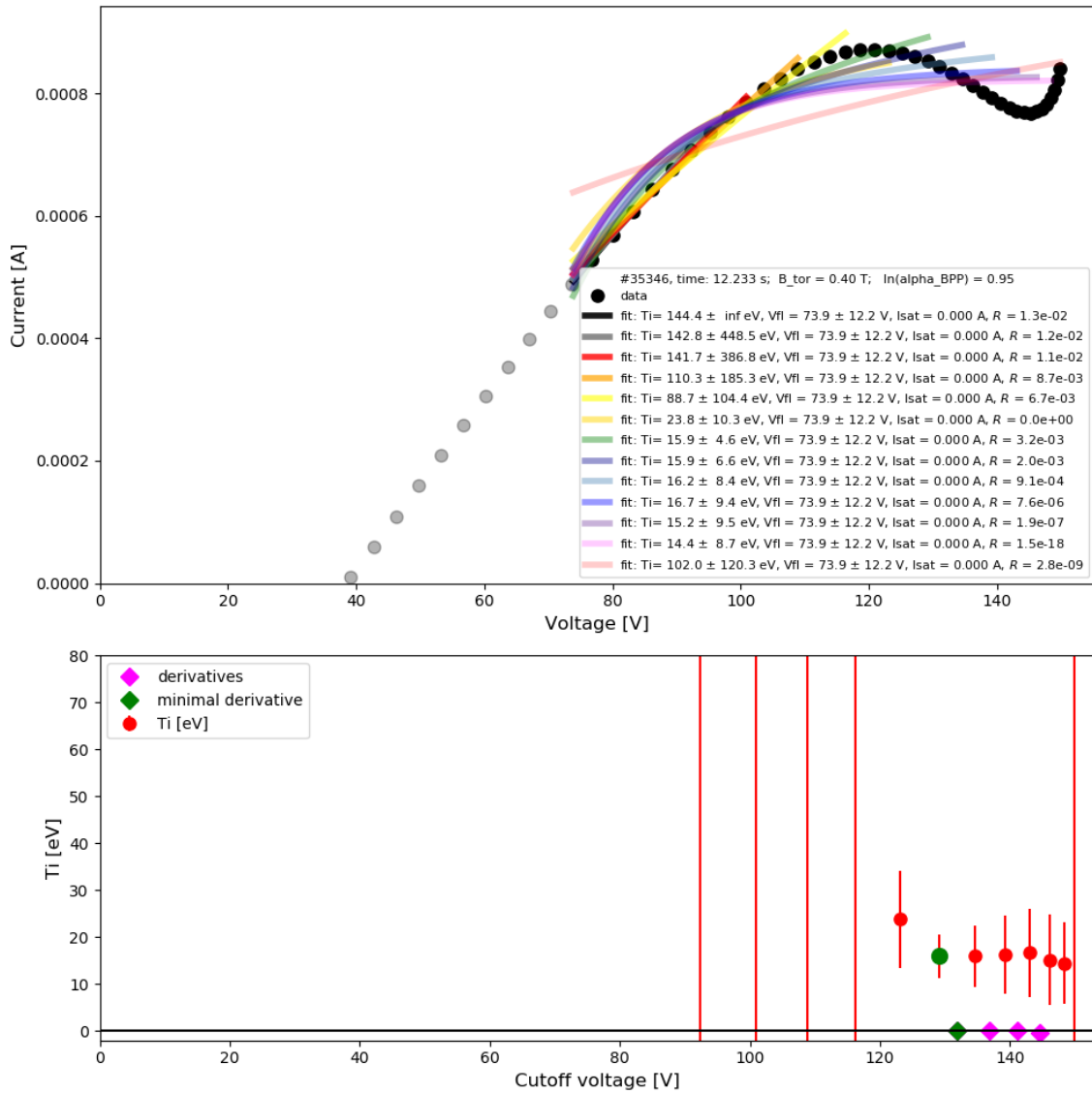


Figure 33: Example of cutoff 4-parameter fit of the electron branch. Top: Graphical representation of the fitting routine. Bottom: Summary of fitting results and their derivatives. Green color marks the resulting  $T_i$  and the lowest derivative, shot: 35346



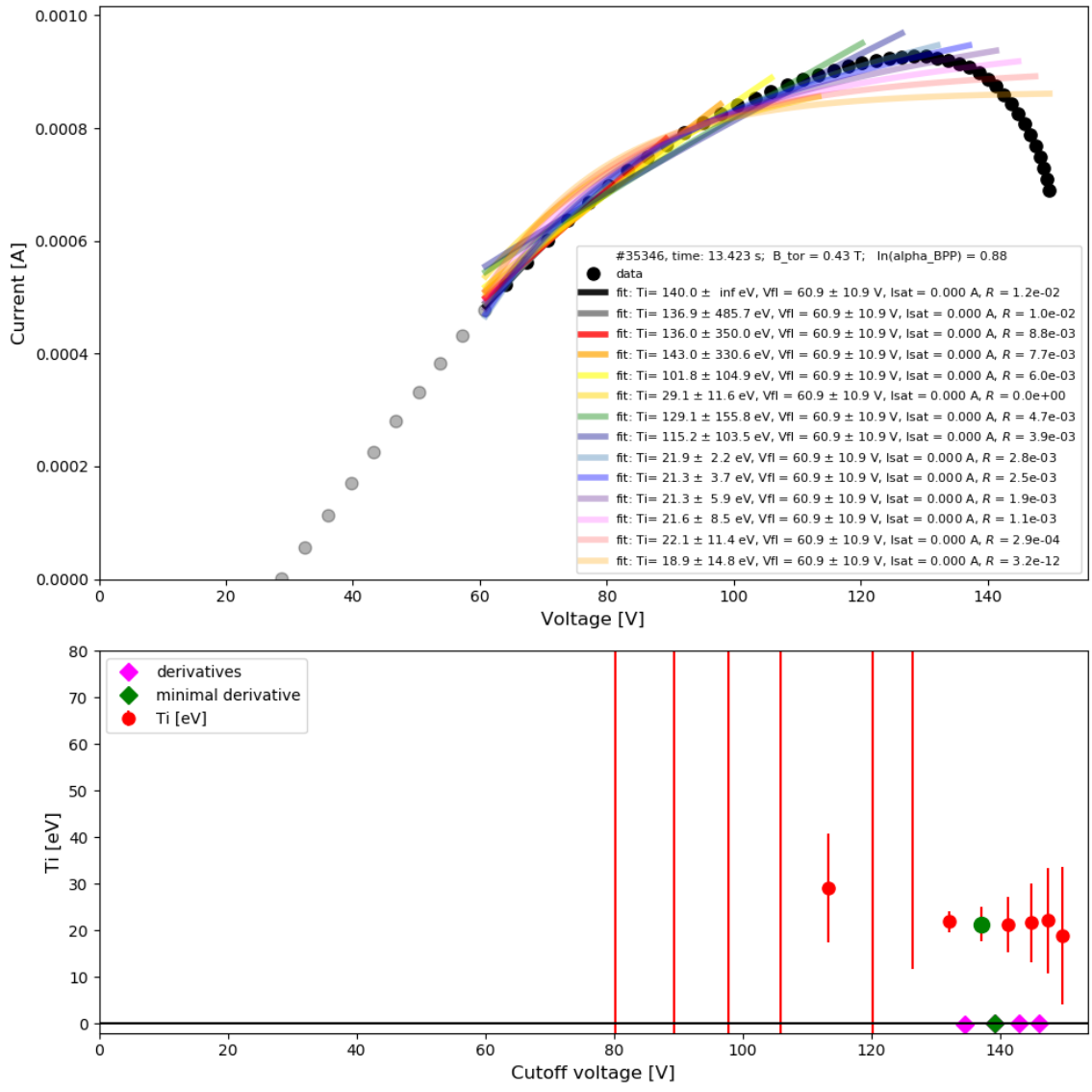


Figure 34: Example of cutoff 4-parameter fit of the electron branch. Top: Graphical representation of the fitting routine. Bottom: Summary of fitting results and their derivatives. Green color marks the resulting  $T_i$  and the lowest derivative, shot: 35346

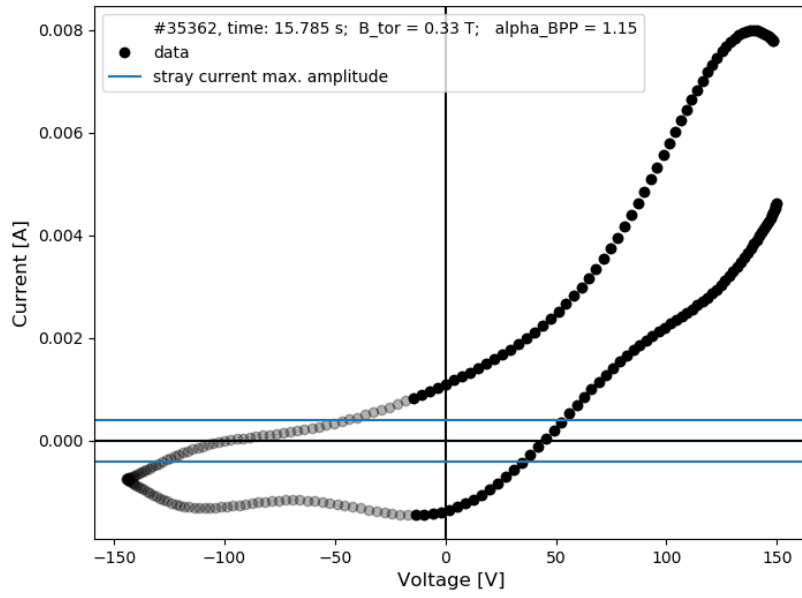


Figure 35: Example of IV-characteristic hysteresis, shot: 353462

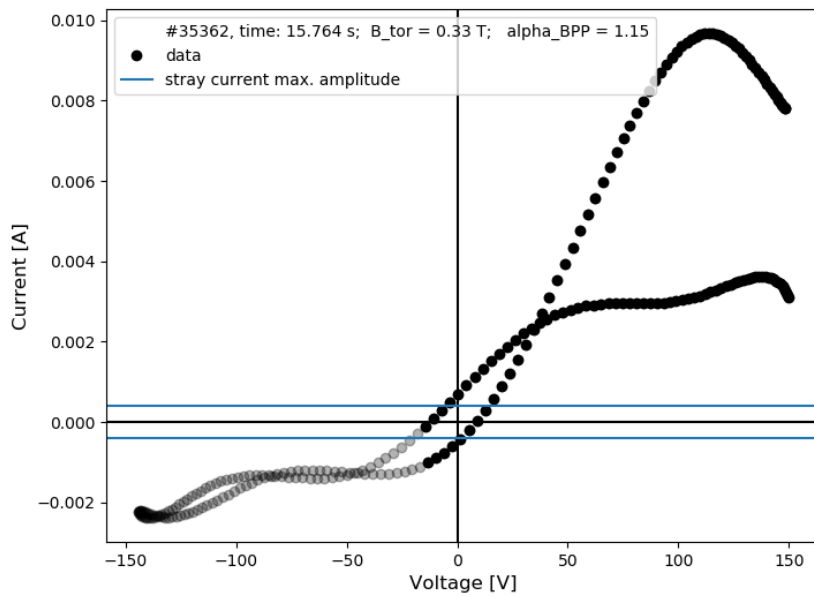


Figure 36: Example of IV-characteristic hysteresis, shot: 353462

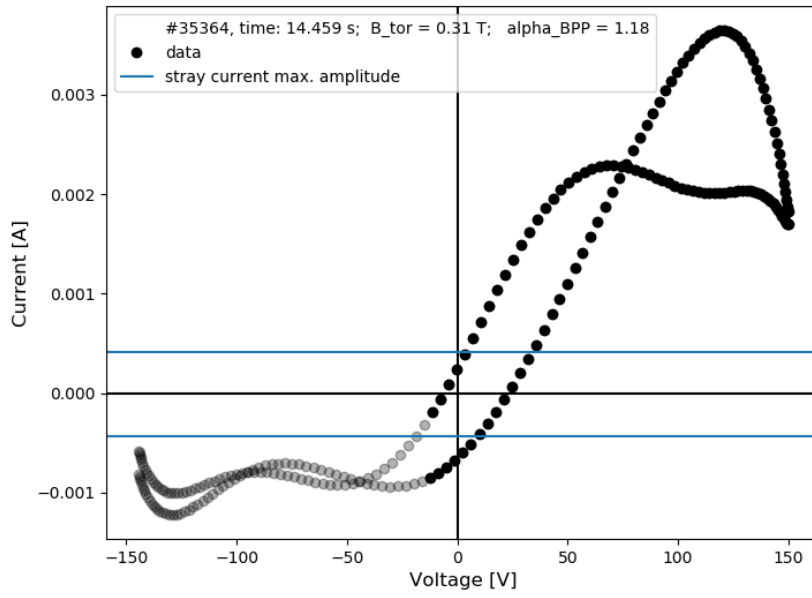


Figure 37: Example of IV-characteristic hysteresis, shot: 353464

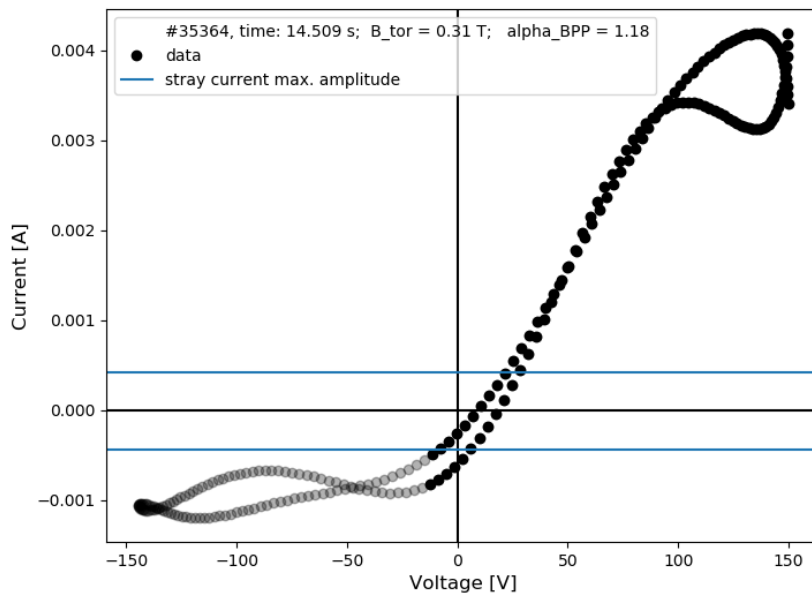


Figure 38: Example of IV-characteristic hysteresis, shot: 353464

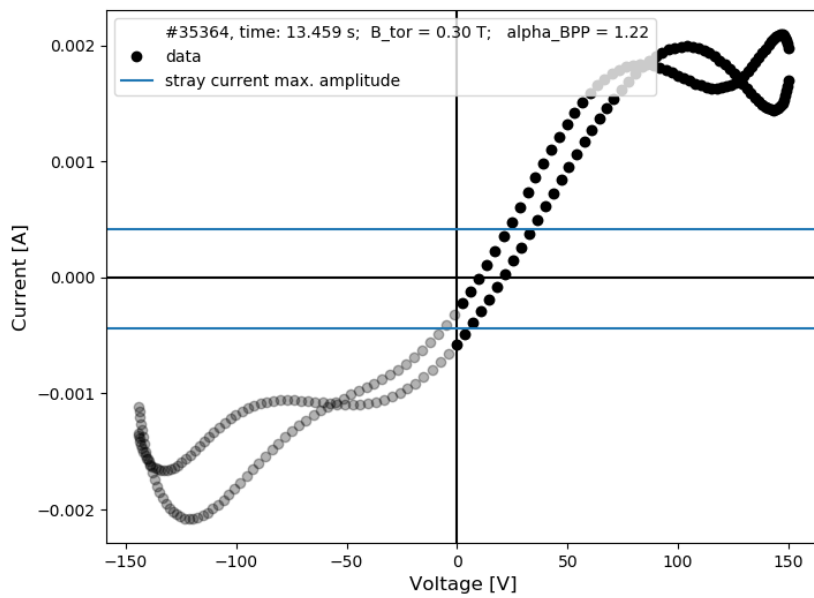


Figure 39: Example of IV-characteristic hysteresis, shot: 353464